

SimpleClick: Interactive Image Segmentation with Simple Vision Transformers

Qin Liu, Zhenlin Xu, Gedas Bertasius, Marc Niethammer
University of North Carolina at Chapel Hill

<https://github.com/uncbiag/SimpleClick>

Abstract

Click-based interactive image segmentation aims at extracting objects with limited user clicking. Hierarchical backbone is the de-facto architecture for current methods. Recently, the plain, non-hierarchical Vision Transformer (ViT) has emerged as a competitive backbone for dense prediction tasks. This design allows the original ViT to be a foundation model that can be finetuned for the downstream task without redesigning a hierarchical backbone for pretraining. Although this design is simple and has been proven effective, it has not yet been explored for interactive segmentation. To fill this gap, we propose the first plain-backbone method, termed as SimpleClick due to its simplicity in architecture, for interactive segmentation. With the plain backbone pretrained as masked auto-encoder (MAE), SimpleClick achieves state-of-the-art performance without bells and whistles. Remarkably, our method achieves **4.15** NoC@90 on SBD, improving **21.8%** over previous best result. Extensive evaluation of medical images highlights the generalizability of our method. We also provide a detailed computation analysis for our method, highlighting its availability as a practical annotation tool.

1. Introduction

Interactive image segmentation aims at obtaining high-quality pixel-level segmentation with limited user interaction such as clicking. It has been widely applied to annotate large-scale image datasets, which drive the success of deep models in various applications, including video understanding [4, 47], self-driving [6], and medical imaging [29, 38]. Much research has been devoted to exploring interactive image segmentation with different interaction types, such as bounding boxes [45], polygons [1], clicks [40], scribbles [43], and their combinations [49]. Among them, click-based approaches have evolved as the mainstream mainly due to their simplicity.

Recent advance of click-based approaches mainly lies in two orthogonal directions. The first is to develop more effective backbone networks; the other is to explore more elab-

NoC@90 on SBD dataset

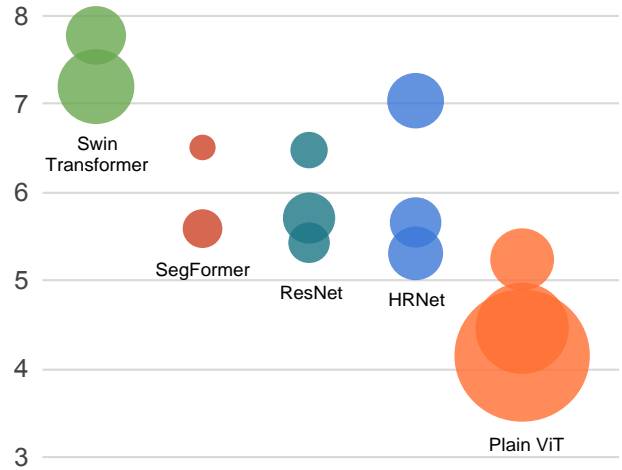


Figure 1. **Interactive segmentation results on SBD [18].** The metric “NoC@90” denotes the number of clicks required to obtain 90% IoU. Each bubble’s area is proportional to FLOPs of a variant in a model family (Tab. 5). We show that plain ViTs outperform all hierarchical backbones for interactive image segmentation.

orated refinement modules built upon the backbone. For the former direction, different hierarchical backbones, including both ConvNets [27, 40] and ViTs [9, 30], have been developed for interactive segmentation. For the latter direction, various refinement modules, including local refinement [9, 27] and click imitation [31], have been proposed to further boost the performance. In this work, we delve into the former direction and focus on exploring plain backbone for interactive segmentation.

Hierarchical backbone is the predominant architecture for current interactive segmentation methods. This design deeply roots in ConvNets, represented by ResNet [20], and is adopted by ViTs, represented by Swin Transformer [32]. The motivation of hierarchical backbone stems from the locality of convolution operation, leading to insufficient receptive field size for the model. To increase the receptive field size, ConvNets have to progressively downsample feature maps and thus capture more global contextual information.

Therefore, they often need an in-network feature pyramid such as FPN [25] to aggregate multi-scale representations for high-quality segmentation. However, the foundation no longer holds for plain ViT, in which the global information is captured since the first self-attention block. Because all feature maps in the ViT are of the same resolution, the motivation of FPN-like feature pyramid is also lost. The above reasoning is supported by a recent finding that plain ViT can serve as a strong backbone for object detection [23], aided by MAE [19] pretraining and window attention (without shifting) for finetuning. This finding also indicates a general-purpose ViT backbone that decouples pretraining from finetuning and enjoys the benefits from the readily available pre-trained MAE models. However, although this design is simple and has been proven effective, it has not yet been explored in interactive segmentation.

In this work, we propose `SimpleClick`, the first plain-backbone method for interactive image segmentation. The core of `SimpleClick` is a plain backbone that maintains a queue of single-scale feature maps throughout. We *only* take the last feature map from the plain backbone to build a simple feature pyramid for segmentation, largely decoupling the general-purpose backbone from the segmentation-specific modules. To make `SimpleClick` more efficient, we use a light-weight MLP decoder to transform the simple feature pyramid into segmentation (see Sec. 3 for details).

We extensively evaluated our method on **10** public benchmarks, including both natural and medical image datasets. With the plain backbone pre-trained as MAE, our method achieved **4.15** NoC@90 on SBD, outperforming previous best method by **21.8%** without complex FPN design and local refinement. We demonstrated the generalizability of our method by out-of-domain evaluation on medical images. We further analyzed the computation efficiency of `SimpleClick`, highlighting its availability as a practical annotation tool. Our main contributions are as follows:

- We propose `SimpleClick`, the first plain-backbone method for interactive image segmentation.
- `SimpleClick` can achieve state-of-the-art performance on natural images and show strong generalizability on medical images, without finetuning.
- We compare `SimpleClick` with existing state-of-the-arts on computation efficiency, highlighting its availability as a practical annotation tool.

2. Related Work

Interactive Image Segmentation Interactive image segmentation is a longstanding vision problem that remains unsolved. Early works [5, 14, 16, 37] tackle this problem by optimizing a graph defined over image pixels. However, these traditional methods only focus on low-level image features, and therefore suffer from tackling complex objects.

Thriving on large datasets as effective feature extractors, ConvNets [9, 27, 31, 33, 40, 43, 45, 46, 49] have surpassed traditional methods and evolved as the dominant architecture for interactive segmentation. Meanwhile, various interaction types have been proposed, such as bounding boxes [45], polygons [1], clicks [40], and scribbles [43]. Click-based approaches are the mainstream due to their simplicity and well-established training and evaluation protocols. Xu *et al.* [46] first proposes a click simulation strategy that has been adopted by follow-up works [9, 31, 40]. DEXTR [33] extracts a target object with its four extreme points. FCA-Net [28] demonstrates the critical role of the first click for better segmentation. Recently, ViTs have been applied to interactive segmentation. FocalClick [9] adopts SegFormer [44] as the backbone network for interactive segmentation and achieves state-of-the-art with high computation efficiency. iSegFormer [44] adopts Swin Transformer [32] as the backbone and applies to medical images. Besides the contribution on backbones, some works devoted to exploring elaborated refinement modules built upon the backbone. FocalClick [9] and FocusCut [27] propose similar local refinement modules for high-quality segmentation. PseudoClick [31] proposes a click-imitation mechanism by estimating the next-click to further reduce human annotation cost. Our method adopts clicking as the interaction. It differs from all previous click-based methods in its plain, non-hierarchical backbone.

Vision Transformers for Segmentation Recently, ViT-based approaches [15, 22, 41, 44] have emerged with competitive performance on segmentation task compared to ConvNets. The original ViT [11] is a non-hierarchical architecture that only maintains single-scale feature maps throughout. SETR [51] and Segmenter [41] use the original ViT as the encoder for semantic segmentation. To allow for more efficient segmentation, Swin Transformer [32] reintroduces hierarchy into the original ViT architecture using shifted window attention, leading to a highly efficient hierarchical ViT backbone. HRFormer [48] uses multi-resolution parallel design [42] to learn high-resolution representations. SegFormer [44] designs hierarchical feature representation for the original ViT using overlapped patch merging, combined with a light-weight MLP decoder for efficient segmentation. HRViT [15] integrates high-resolution multi-branch architecture with ViTs to learn multi-scale representations. Recently, the original ViT is reintroduced as a strong and efficient backbone for semantic segmentation [7] and object detection [23], with the aid of MAE [19] pretraining and window attention for finetuning. This finding indicates a general-purpose ViT backbone, which decouples pretraining from finetuning and enjoys the benefits from the readily available pre-trained MAE models. Inspired by this finding, we explore plain-ViT as the backbone network, along with other task-specific modules, for interactive segmentation.

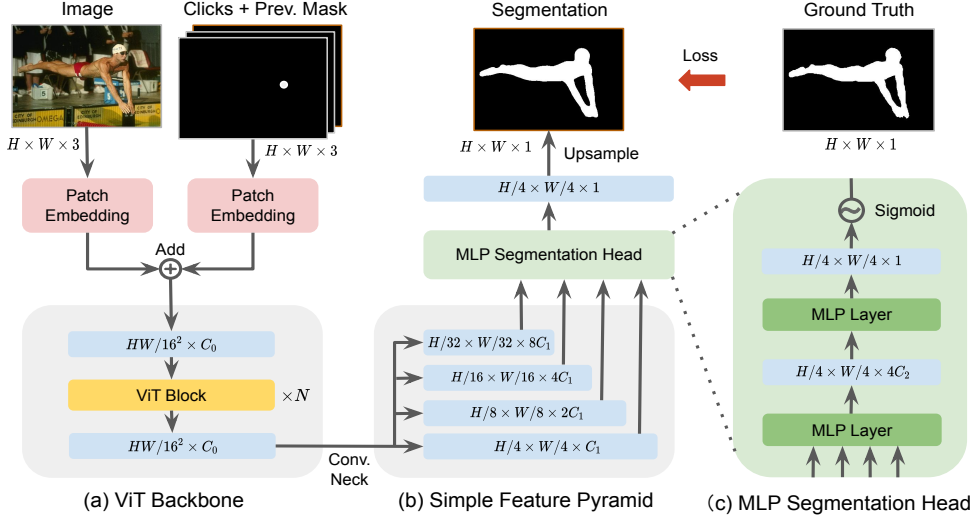


Figure 2. **SimpleClick overview.** Our method consists of three main modules: (a) a plain ViT backbone that maintains a queue of single-scale feature maps; (b) a multi-scale simple feature pyramid that is generated from the *last* feature map of the backbone by four parallel convolution or deconvolution layers; (c) a light-weight MLP decoder for segmentation. We also use previous segmentation as input to allow for refining from existing mask. The user clicks are encoded as a two-channel disk map, combined with the previous segmentation as input. The positional encoding is not shown for brevity.

3. Method

We aim to adapt a plain-ViT backbone with *minimal* modifications for interactive segmentation. In Sec. 3.1, we first introduce the adaptation of plain-ViT backbone, as well as other main modules. In Sec. 3.2, we describe the training and inference details of our method. We conclude in Sec. 3.3 with implementation details and discussion.

3.1. Network Architecture

Adaptation of Plain-ViT Backbone We use plain ViT [11] as our backbone network, which only maintains single-scale feature maps throughout. The patch embedding layer divides the input image into non-overlapping fixed-size patches (e.g. 16×16 for ViT-B), each patch is flattened and linearly projected to a fixed-length vector (e.g. 768 for ViT-B). The resulting sequence of vectors is feed into a queue of Transformer blocks (e.g. 12 for ViT-B) for self-attention. Specifically, we implement SimpleClick with three backbones: ViT-B, ViT-L, and ViT-H (Tab. 1 shows the parameters of the three backbones). The three backbones were pretrained on ImageNet-1k as MAE [19]. We adapt the pretrained backbones on higher-resolution inputs during finetuning using non-shifting window attention aided by a few Transformers blocks (e.g. 2 for ViT-B) for global propagation, following the strategy introduced in ViTDet [23]. Since the last feature map undergoes all the attention blocks, it should has the strongest representation. Therefore, we only use the last feature map to build a multi-scale simple feature pyramid.

Model↓ Module→	ViT Backbone	Conv. Neck	MLP Head
Ours-ViT-B	83.0 (89.3%)	9.0 (9.7%)	0.9 (1.0%)
Ours-ViT-L	290.8 (94.3%)	16.5 (5.3%)	1.1 (0.4%)
Ours-ViT-H	604.0 (95.7%)	25.8 (4.1%)	1.3 (0.2%)

Table 1. **Number of parameters (unit: million)** for our models. The ViT backbone takes the lion’s share for each model.

Simple Feature Pyramid For hierarchical backbone, feature pyramid is commonly produced by a top-down in-network with lateral connections [25] to combine features from different stages. For plain backbone, feature pyramid can be produced in a much simpler way: only applying a set of parallel convolutional or deconvolutional layers on the last feature map of the backbone. As shown in Fig. 2, given the input ViT feature map, a multi-scale feature map can be produced by four convolutions with different strides. The effectiveness of this simple feature pyramid is first demonstrated in ViTDet [23] for object detection. We also find this simple feature pyramid is sufficient for our method to achieve superior performance on interactive segmentation. Note that this module only takes a tiny portion of the model parameters, as shown in Tab. 1. In ViTDet [23], the authors also compared with two other FPN variants for plain backbone, showing the superiority of the simple feature pyramid. In this work, we will compare with another two FPN variants that can be built for plain backbone, as shown in Fig. 6.

All-MLP Segmentation Head We implement a lightweight segmentation head using only MLP layers. It takes in the

simple feature pyramid and produces a segmentation probability map of scale $1/4$, followed by a upsampling operation to recover the original resolution. Note that this segmentation head avoids computationally demanding components and only takes up to 1% of model parameters (Tab. 1). The key insight is that with a powerful backbone pre-trained as MAE, a lightweight segmentation head is enough for the interactive segmentation task. The proposed all-MLP segmentation head works in three steps. *First*, each feature map from the simple feature pyramid goes through an MLP layer to transform to a same channel dimension (*i.e.* C_2 in Fig. 2). *Second*, all feature maps will be upsampled to the same resolution (*i.e.* $1/4$ in Fig. 2) for concatenation. *Third*, the concatenated features will be fused by another MLP layer to produce a single-channel feature map, followed by Sigmoid function for a probability map.

Other Modules The user clicks are encoded in a two-channel disk map, one for positive clicks and the other for the negative clicks. The positive clicks should to be placed on the foreground, while the negative ones should be placed on the background. The previous segmentation and the two-channel click map are concatenated as a three-channel map for the patch embedding. Two separate patch embedding layers operate on the image and the concatenated three-channel map, respectively. The two inputs are patchified, flattened, and projected to two vector sequences of same dimension, followed by an element-wise addition before feeding into the Transformer blocks.

3.2. Training and Inference Settings

Pretraining The ViT models are pretrained on ImageNet-1K [10] as MAE [19]. In MAE pretraining, the ViT models reconstruct the randomly masked pixels of images by learning the representation. This simple self-supervised approach turns out to be an efficient and scalable way to pre-train ViT models. Our method enjoys the benefit from the readily available pretrained ViT models. In this work, we simply use the pretrained weights released by MAE.

Finetuning With the pretrained backbone, we finetune our model on the interactive segmentation task. The training pipeline can be briefly described as follows. *First*, we automatically simulate clicks based on the current segmentation and ground truth, without a human-in-the-loop providing the clicks. Specifically, we use a combination of random and iterative click simulation strategies, inspired by RITM [40]. The random click simulation strategy generates clicks in parallel, without considering the order between the clicks. The iterative click simulation strategy generates clicks iteratively-the next click should be placed on the erroneous region of a prediction using previous clicks. This strategy is more like the human clicking behavior. *Second*, we incorporate the segmentation from the previous interaction as an additional input for the backbone, further

improving the segmentation quality. This also allows our method to refine from existing segmentation, which is an indispensable feature for a practical annotation tool. We use normalized focal loss [40] (NFL) to train all our models. Previous works [9, 40] show that NFL converges faster and achieves better performance than the widely used binary cross entropy loss in the interactive segmentation task. Similar training pipelines have been proposed by RITM [40] and its follow-up works [8, 9, 31].

Inference There are two inference modes: automatic evaluation and human evaluation. For automatic evaluation, we use a deterministic click simulation strategy using the ground truth, which is the standard evaluation protocol. For human evaluation, a human-in-the-loop will provide clicks based on his/her subjective evaluation of current segmentation results.

3.3. Discussion

Hierarchical ViT with MAE Recently, HiViT [50] shows that hierarchical ViT can also be pretrained as MAE. However, comparing with hierarchical ViT, plain ViT has its strengths in simplicity and few image prior such as locality. In light of this, we believe the plain ViT is more suitable as a foundation model, which can be finetuned in various downstream tasks.

Implementation We do not aim to propose new components. Instead, we hope to draw new insights by applying plain ViTs with minimal modification for interactive segmentation. This design enjoys the readily available pretrained ViT models [19]. The implementation is not complicated thanks to the simplicity of our method. One of the major technical issue might be how to efficiently finetune the plain backbone on higher-resolution images. ViTDet [23] has explored an effective solution: non-shifting window attention aided by a few blocks for cross-window propagation. We adopt this implementation and find it works quite well for interactive segmentation. We also explored other solutions for efficient attention. However, none of them works better than the window attention.

4. Experiments

Datasets We conducted experiments on 10 public datasets including 7 natural image datasets and 3 medical datasets.

- **GrabCut** [37]: It contains 50 images (50 instances), each with clear foreground and background difference.
- **Berkeley** [34]: It contains 96 images (100 instances) and shares a small portion of images with GrabCut.
- **DAVIS** [36]: It contains 50 videos, but we only use the same 345 frames as [9, 27, 31, 40] used for evaluation.
- **Pascal VOC** [12]: Following previous works, we only test on the validation set (1449 images, 3427 instances).

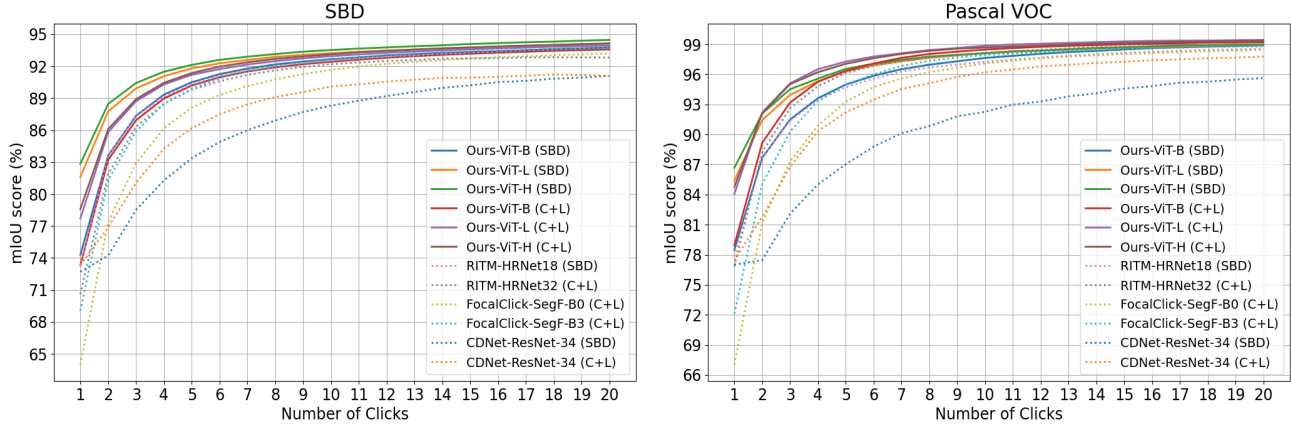


Figure 3. **Convergence analysis** for the top two largest benchmarks: SBD [18] and Pascal VOC [12]. Models are trained on either SBD [18] or COCO [26]+LVIS [17] (denoted as C+L). The metric is mIoU@ k given k clicks.

Method	Backbone	GrabCut		Berkeley		SBD		DAVIS		Pascal VOC	
		NoC85	NoC90	NoC85	NoC90	NoC85	NoC90	NoC85	NoC90	NoC85	NoC90
♪ DIOS [46] _{CVPR16}	FCN	-	6.04	-	8.65	-	-	-	12.58	6.88	-
♪ FCA-Net [28] _{CVPR20}	ResNet-101	-	2.08	-	3.92	-	-	-	7.57	2.69	-
♪ LD [24] _{CVPR18}	VGG-19	3.20	4.79	-	-	7.41	10.78	5.05	9.57	-	-
♪ BRS [21] _{CVPR19}	DenseNet	2.60	3.60	-	5.08	6.59	9.78	5.58	8.24	-	-
♪ f-BRS [39] _{CVPR20}	ResNet-101	2.30	2.72	-	4.57	4.81	7.73	5.04	7.41	-	-
♪ RITM [40] _{Preprint21}	HRNet-18	1.76	2.04	1.87	3.22	3.39	5.43	4.94	6.71	2.51	3.03
♪ CDNet [8] _{ICCV21}	ResNet-34	1.86	2.18	1.95	3.27	5.18	7.89	5.00	6.89	3.61	4.51
♪ PseudoClick [31] _{ECCV22}	HRNet-18	1.68	2.04	1.85	3.23	3.38	5.40	4.81	6.57	2.34	2.74
♪ FocalClick [9] _{CVPR22}	HRNet-18s	1.86	2.06	-	3.14	4.30	6.52	4.92	6.48	-	-
♪ FocalClick [9] _{CVPR22}	SegF-B0	1.66	1.90	-	3.14	4.34	6.51	5.02	7.06	-	-
♪ FocusCut [27] _{CVPR22}	ResNet-50	1.60	1.78	1.85 [†]	3.44	3.62	5.66	5.00	6.38	-	-
♪ FocusCut [27] _{CVPR22}	ResNet-101	1.46	1.64	1.81 [†]	3.01	3.40	5.31	4.85	6.22	-	-
♪ Ours	ViT-B	1.40	1.54	1.44	2.46	3.28	5.24	4.10	5.48	2.38	2.81
♪ Ours	ViT-L	1.38	1.46	1.40	2.33	2.69	4.46	4.12	5.39	1.95	2.30
♪ Ours	ViT-H	1.32	1.44	1.36	2.09	2.51	4.15	4.20	5.34	1.88	2.20
♪ RITM [40] _{Preprint21}	HRNet-32	1.46	1.56	1.43	2.10	3.59	5.71	4.11	5.34	2.19	2.57
♪ CDNet [8] _{ICCV21}	ResNet-34	1.40	1.52	1.47	2.06	4.30	7.04	4.27	5.56	2.74	3.30
♪ PseudoClick [31] _{ECCV22}	HRNet-32	1.36	1.50	1.40	2.08	3.46	5.54	3.79	5.11	1.94	2.25
♪ FocalClick [9] _{CVPR22}	SegF-B0	1.40	1.66	1.59	2.27	4.56	6.86	4.04	5.49	2.97	3.52
♪ FocalClick [9] _{CVPR22}	SegF-B3	1.44	1.50	1.55	1.92	3.53	5.59	3.61	4.90	2.46	2.88
♪ Ours	ViT-B	1.38	1.48	1.36	1.97	3.43	5.62	3.66	5.06	2.06	2.38
♪ Ours	ViT-L	1.32	1.40	1.34	1.89	2.95	4.89	3.26	4.81	1.72	1.96
♪ Ours	ViT-H	1.38	1.50	1.36	1.75	2.85	4.70	3.41	4.78	1.76	1.98

Table 2. **Comparison with previous results.** We evaluate on five benchmarks: GrabCut [37], Berkeley [34], SBD [18], DAVIS [36], and Pascal VOC [12]. The training sets for our models are either SBD or COCO [26]+LVIS [17] (denoted as C+L). The best results are set in bold. ♪ denotes model trained on Pascal; ♪ denotes model trained on SBD; ♪ denotes model trained on C+L; † denotes number reproduced by the released or retrained models. Our models outperform state-of-the-arts on all the benchmarks.

- **SBD [18]:** It contains 8498 training images (20172 instances) and 2857 validation images (6671 instances). We train our model on the training set and evaluate on the validation set.
- **COCO [26]+LVIS [17] (C+L):** COCO contains 118K training images (1.2M instances); LVIS shares the same images but has much higher segmentation qual-

ity. We combine the two datasets for training.

- **ssTEM [13]:** It contains two image stacks, each contains 20 images. We use the same stack as [31] used.
- **BraTS [3]:** It contains 369 MR volumes; we test on the same 369 frames (369 instances) as [31] used.
- **OAIZIB [2]:** It contains 507 MR volumes; we test on the same 150 frames (300 instances) as [30] used.

Evaluation Metrics Following previous works [9, 27, 31, 39, 40], we automatically simulate user clicks based on the current segmentation error by comparing current segmentation with ground truth. In this simulation, the next click will be put on the center of the region with the largest error. We use the Number of Click (NoC) as the evaluation metric to calculate the number of clicks required to achieve a target Intersection over Union (IoU). We set two target IoUs: 85% and 90%, represented by NoC%85 and NoC%90 respectively. The maximum number of clicks for each instance is set to 20. We also use the average IoU given k clicks (mIoU@ k) as the evaluation metric to measure the segmentation quality given fixed number of clicks.

Implementation Details We implement SimpleClick models in Python, using PyTorch [35]. We implement three SimpleClick models based on three vanilla ViT models (*i.e.* ViT-B, ViT-L, and ViT-H). The three backbone models are pre-trained on ImageNet-1k as MAE; we download the weights directly from the repository provided by MAE. We train our models on either SBD or COCO+LVIS with 55 epochs; the initial learning rate is set to 5×10^{-5} and will decrease to 5×10^{-6} after the epoch 50. We set the batch size to 140 for ViT-Base, 72 for ViT-Large, and 32 for ViT-Huge to suit the GPU memory—all our models on four NVIDIA RTX A6000 GPUs. The data augmentation techniques include: random resizing (scale range from 0.75 to 1.25), random flipping and rotation, random brightness contrast, and random cropping. Though the ViT backbone was pretrained on image size 224×224 , we finetune on 448×448 with non-shifting window attention for better performance. We optimize using Adam with $\beta_1 = 0.9$, $\beta_2 = 0.999$. Please refer to our code for additional details.

4.1. Comparison with Previous Results

Tab. 2 shows the comparison results with previous state-of-the-arts. When trained on the SBD dataset, our model achieves best results on all benchmarks. Remarkably, on the SBD validation set, our model achieves 4.15 NoC@90, outperforming previous best score by 21.8%. Since SBD contains the largest number of instances, this improvement is convincing. When trained on the COCO+LVIS dataset, our model also achieves the best results on all benchmarks. Note the DAVIS dataset contains high-quality ground truth for instances, our model still outperforms other methods without using local refinement, as adopted by FocalClick [9]. Fig. 3 shows that our method converges better than other methods with sufficient clicks, leading to fewer failure cases as indicated in Fig. 4. Our results are shown in solid lines, while previous results are shown in dashed lines. We only show results on the SBD and Pascal VOC, which are the top two largest datasets. We shall provide results on other benchmarks in the supplementary materials.

Model	ssTEM mIoU@10	BraTS mIoU@10 / 20	OAIZIB mIoU@10 / 20
♪ RITM-H18	93.15	87.05 / 90.47	71.04 / 78.52
♪ CDNet-RN-34	66.72	58.34 / 82.07	38.07 / 61.17
♪ RITM-H32	94.11	88.34 / 89.25	75.27 / 75.18
♪ CDNet-RN-34	88.46	80.24 / 86.63	63.19 / 74.21
♪ F-Click-SF-B0	92.62	86.02 / 90.74	74.08 / 79.14
♪ F-Click-SF-B3	93.61	88.62 / 90.58	75.77 / 80.08
♪ Ours-ViT-B	93.72	86.98 / 90.67	76.05 / 79.61
♪ Ours-ViT-L	94.34	88.43 / 90.84	77.34 / 79.97
♪ Ours-ViT-H	94.08	88.98 / 91.00	77.50 / 80.10

Table 3. **Out-of-domain evaluation** on three medical image datasets: ssTEM [13], BraTS [3], and OAIZIB [2]. Our models generalize well on medical images even without finetuning.

FP design	frozen ViT	ViT-B		ViT-L	
		SBD	Pascal	SBD	Pascal
(a) simple FP	✓	11.48	6.93	9.75	5.59
(a) simple FP	✗	5.24	2.53	4.46	2.15
(b) simpler FP	✗	6.56	2.80	5.53	2.48
(c) parallel FP	✗	7.21	3.09	6.26	2.79

Table 4. **Ablation study** on backbone finetuning and feature pyramid (FP) design. By default, the ViT backbone will be finetuned along with other modules. As an ablation, its pretrained weights will be frozen during finetuning. By default, we use the simple feature pyramid design (*i.e.* (a) in Fig. 6). We compare it with other designs (*i.e.* (b) and (c) in Fig. 6). The metric is NoC@90.

4.2. Out-of-Domain Evaluation on Medical Images

In this section, we evaluate the generalizability of our models on three medical image datasets: ssTEM, BraTS, and OAIZIB. Tab. 3 reports the evaluation results on the three datasets. Fig. 5 shows the convergence analysis on BraTS and OAIZIB. Overall, our models generalize well to medical images, without finetuning. The models trained on larger datasets (*i.e.* COCO+LVIS) generalize better than models trained on smaller datasets (*i.e.* SBD). Note that medical images are significantly different than natural images; objects in medical images are unseen objects for our models.

4.3. Ablation Study

In this section, we ablate the backbone finetuning and feature pyramid design. Tab. 4 shows the ablation results. By default, we finetune the backbone, along with other modules, during finetuning. As an ablation, we freeze the backbone during finetuning, leading to significant worse performance as shown in Tab. 4. This ablation is explainable because the ViT backbone takes the lion’s share of model parameters (Tab. 1). For the second ablation, we compare the default simple feature pyramid design (*i.e.* (a) in Fig. 6) with two variants (*i.e.* (b) and (c) in Fig. 6). First, we observe that the multi-scale representation matters for the feature

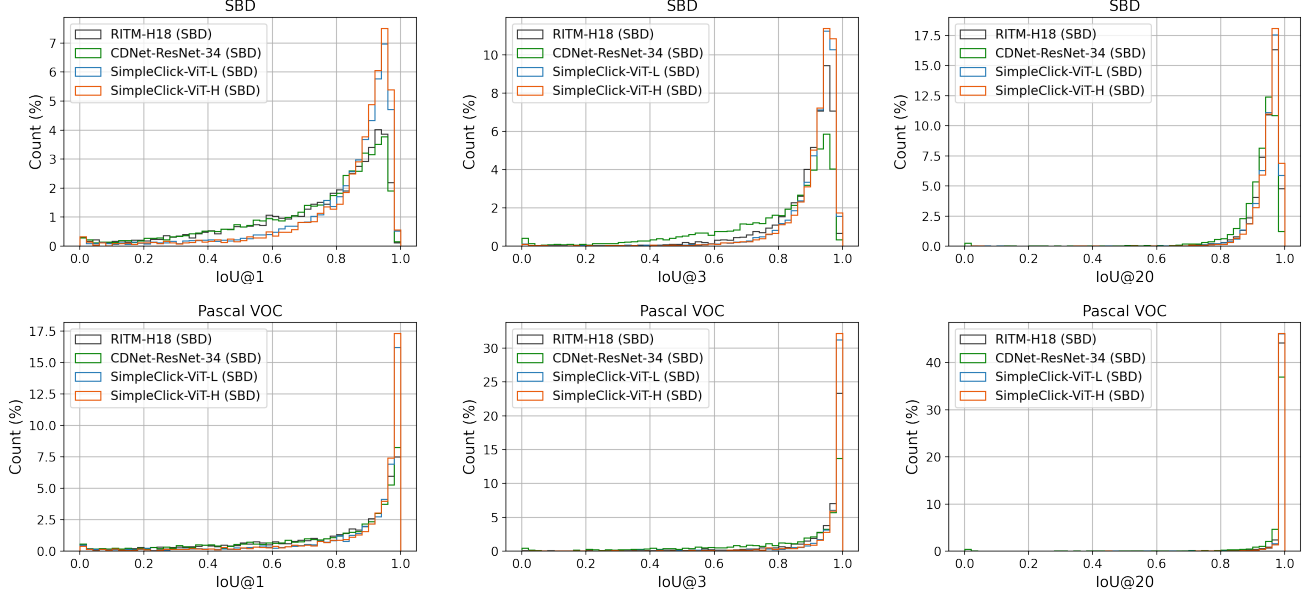


Figure 4. **Histogram analysis for IoU@k** given $k=1, 3, 20$ clicks. We report results on the SBD [18] and Pascal VOC [12]. All models are trained on SBD.

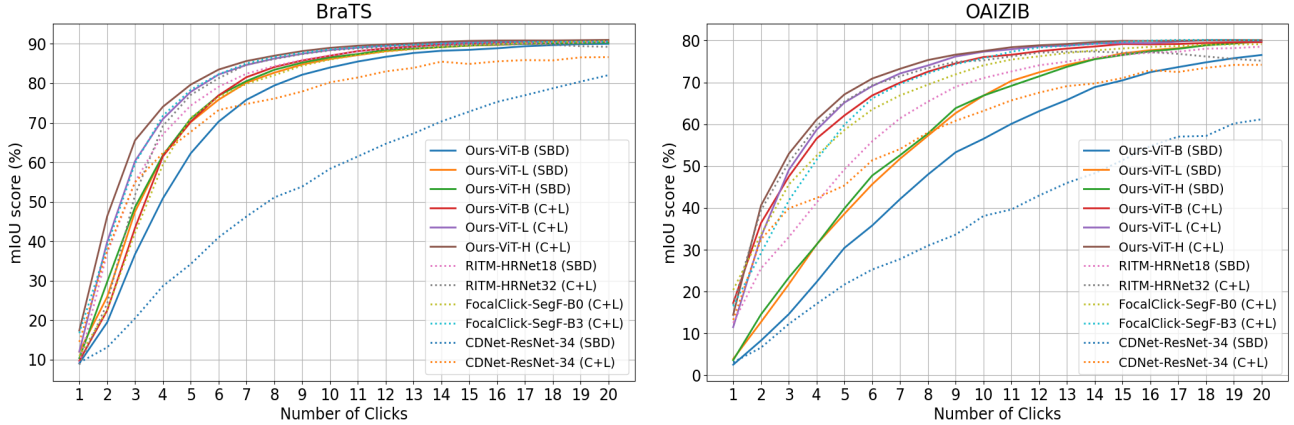


Figure 5. **Convergence analysis** for two medical image datasets: BraTS [3] and OAIZIB [2]. Models are trained on either SBD [18] or COCO [26]+LVIS [17] (denoted as C+L). The metric is mIoU@k given k clicks.

pyramid. By ablating the multi-scale property in the simple feature pyramid, the performance drops considerably. We also notice that the *last* feature map from the backbone is strong enough to build the feature pyramid. The parallel feature pyramid generated by multi-stage feature maps from the backbone does not surpass the simple feature pyramid that only uses the *last* feature map of the backbone.

4.4. Computation Analysis

Tab. 5 shows the computation comparison for model parameters, FLOPs, GPU memory consumption, and speed; the speed is measured by second per click (SPC). Fig. 1 vi-

sualizes the interactive segmentation performance of methods in terms of FLOPs. In Fig. 1 and Tab. 5, each method is represented by its backbone. For fair comparison, we evaluate all the methods on the same benchmark (*i.e.* GrabCut) and same machine (GPU: NVIDIA RTX A6000, CPU: Intel Silverx2). We only calculate the FLOPs in a single forward pass. For method like FocusCut which requires multiple forward passes for each clicking, the FLOPs may be much higher than reported. Our method takes 448×448 as the fixed input by default. Even for our ViT-H model, the speed (132ms) and memory consumption (3.22G) is enough to meet the requirements of a practical annotation tool.

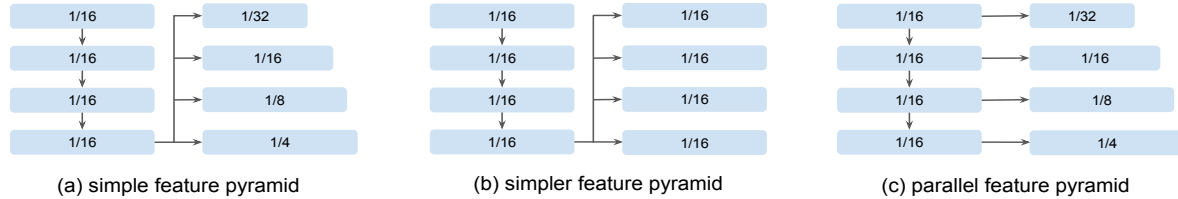


Figure 6. **Three variants of feature pyramid design.** They are: (a) simple feature pyramid; (b) simpler feature pyramid; (c) parallel feature pyramid. We use (a) simple feature pyramid by default. The (b) simpler feature pyramid can be implemented with a single 1×1 convolutional layer.

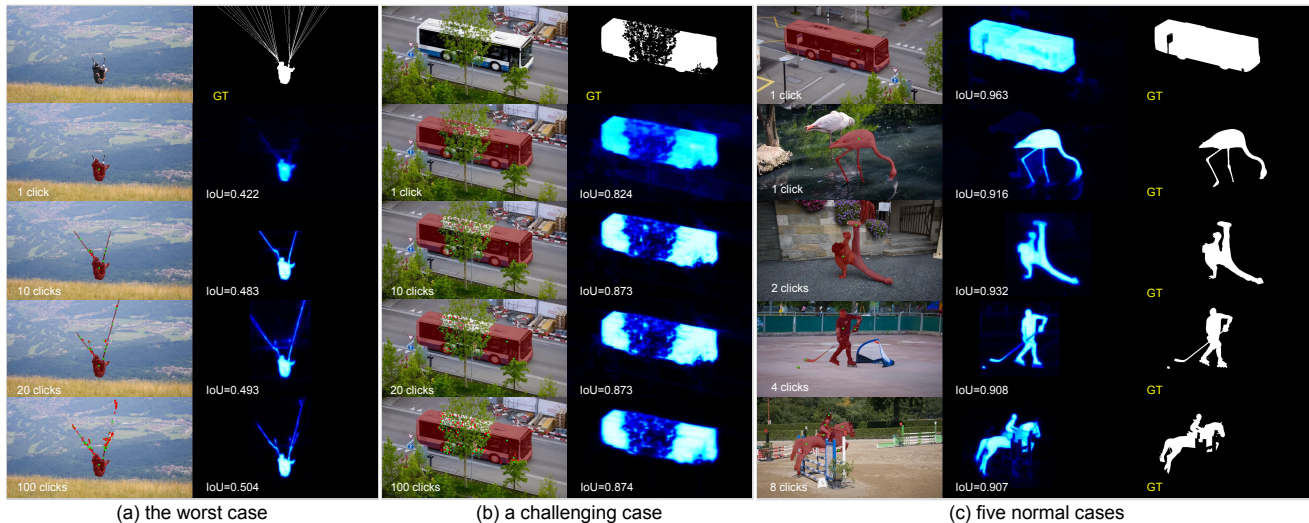


Figure 7. **Qualitative analysis** on DAVIS [36]. We show in this figure: (a) the worst case; (b) a challenging case; (c) five normal cases. The model is SimpleClick-ViT-L trained on C+L dataset. The probability maps are show in blue; the segmentation is overlaid on the original image. The clicks are shown as green (positive click) or red (negative click) dots on the image.

Backbone	Params/M	FLOPs/G	Mem/G	SPC/ms
HR-18s ₄₀₀ [40]	4.22	17.94	0.50	54
HR-18 ₄₀₀ [40]	10.03	30.99	0.52	56
HR-32 ₄₀₀ [40]	30.95	83.12	1.12	86
Swin-B ₄₀₀ [30]	87.44	138.21	1.41	36
Swin-L ₄₀₀ [30]	195.90	302.78	2.14	44
SegF-B0 ₂₅₆ [9]	3.72	3.42	0.10	37
SegF-B3 ₂₅₆ [9]	45.66	24.75	0.32	53
ResN-34 ₃₈₄ [8]	23.47	113.60	0.25	34
ResN-50 ₃₈₄ [27]	40.36	78.82	0.85	331
ResN-101 ₃₈₄ [27]	59.35	100.76	0.89	355
Ours-ViT-B ₂₂₄	96.46	42.44	0.51	34
Ours-ViT-B ₄₄₈	96.46	169.78	0.87	54
Ours-ViT-L ₄₄₈	322.18	532.87	1.72	86
Ours-ViT-H ₄₄₈	659.39	1401.93	3.22	132

Table 5. **Comparison of computation analysis** for model parameters, FLOPs, GPU memory consumption (measured by the maximum GPU memory managed by the Pytorch caching allocator), and speed (measured by second per click). Each method is denoted by its backbone. The input size is denoted by the small number.

5. Limitations

Our method may not be efficient enough to work on low-power devices, especially for the ViT-H model. We believe the coarse-to-fine mechanism proposed in FocalClick [27] should also work for our method to alleviate this issue. However, we do not explore this idea to improve our method. Other than this, our method may fail in some challenging cases (*e.g.* very thin and elongated objects as shown in Fig. 7). We leave the improvement for the future work.

6. Conclusions

We proposed SimpleClick, the first plain-backbone method for interactive segmentation. With the MAE-pretrained backbone, our method achieved state-of-the-art performance and demonstrated strong out-of-domain generalizability on medical images. We also compared SimpleClick with state-of-the-arts on computation efficiency, highlighting the availability of our method as a practical annotation tool.

References

- [1] David Acuna, Huan Ling, Amlan Kar, and Sanja Fidler. Efficient interactive annotation of segmentation datasets with polygon-rnn++. In *Proceedings of the IEEE conference on Computer Vision and Pattern Recognition*, pages 859–868, 2018. [1](#), [2](#)
- [2] Felix Ambellan, Alexander Tack, Moritz Ehlke, and Stefan Zachow. Automated segmentation of knee bone and cartilage combining statistical shape knowledge and convolutional neural networks: Data from the osteoarthritis initiative. *Medical image analysis*, 52:109–118, 2019. [5](#), [6](#), [7](#)
- [3] Ujjwal Baid, Satyam Ghodasara, Suyash Mohan, Michel Bilello, Evan Calabrese, Errol Colak, Keyvan Farahani, Jayashree Kalpathy-Cramer, Felipe C Kitamura, Sarthak Pati, et al. The rsna-asnr-miccai brats 2021 benchmark on brain tumor segmentation and radiogenomic classification. *arXiv preprint arXiv:2107.02314*, 2021. [5](#), [6](#), [7](#)
- [4] Gedas Bertasius and Lorenzo Torresani. Classifying, segmenting, and tracking object instances in video with mask propagation. In *Proceedings of the IEEE/CVF Conference on Computer Vision and Pattern Recognition*, pages 9739–9748, 2020. [1](#)
- [5] Yuri Y Boykov and M-P Jolly. Interactive graph cuts for optimal boundary & region segmentation of objects in ND images. In *Proceedings eighth IEEE international conference on computer vision. ICCV 2001*, volume 1, pages 105–112. IEEE, 2001. [2](#)
- [6] Holger Caesar, Varun Bankiti, Alex H Lang, Sourabh Vora, Venice Erin Liong, Qiang Xu, Anush Krishnan, Yu Pan, Giancarlo Baldan, and Oscar Beijbom. nuscenes: A multi-modal dataset for autonomous driving. In *Proceedings of the IEEE/CVF conference on computer vision and pattern recognition*, pages 11621–11631, 2020. [1](#)
- [7] Wuyang Chen, Xianzhi Du, Fan Yang, Lucas Beyer, Xiaohua Zhai, Tsung-Yi Lin, Huizhong Chen, Jing Li, Xiaodan Song, Zhangyang Wang, et al. A simple single-scale vision transformer for object localization and instance segmentation. *arXiv preprint arXiv:2112.09747*, 2021. [2](#)
- [8] Xi Chen, Zhiyan Zhao, Feiwu Yu, Yilei Zhang, and Manni Duan. Conditional diffusion for interactive segmentation. In *Proceedings of the IEEE/CVF International Conference on Computer Vision*, pages 7345–7354, 2021. [4](#), [5](#), [8](#)
- [9] Xi Chen, Zhiyan Zhao, Yilei Zhang, Manni Duan, Donglian Qi, and Hengshuang Zhao. Focalclick: Towards practical interactive image segmentation. In *Proceedings of the IEEE/CVF Conference on Computer Vision and Pattern Recognition*, pages 1300–1309, 2022. [1](#), [2](#), [4](#), [5](#), [6](#), [8](#)
- [10] Jia Deng, Wei Dong, Richard Socher, Li-Jia Li, Kai Li, and Li Fei-Fei. Imagenet: A large-scale hierarchical image database. In *2009 IEEE conference on computer vision and pattern recognition*, pages 248–255. Ieee, 2009. [4](#)
- [11] Alexey Dosovitskiy, Lucas Beyer, Alexander Kolesnikov, Dirk Weissenborn, Xiaohua Zhai, Thomas Unterthiner, Mostafa Dehghani, Matthias Minderer, Georg Heigold, Sylvain Gelly, et al. An image is worth 16x16 words: Transformers for image recognition at scale. *arXiv preprint arXiv:2010.11929*, 2020. [2](#), [3](#)
- [12] Mark Everingham, Luc Van Gool, Christopher KI Williams, John Winn, and Andrew Zisserman. The pascal visual object classes (voc) challenge. *International journal of computer vision*, 88(2):303–338, 2010. [4](#), [5](#), [7](#)
- [13] Stephan Gerhard, Jan Funke, Julien Martel, Albert Cardona, and Richard Fetter. Segmented anisotropic sstem dataset of neural tissue. *figshare*, pages 0–0, 2013. [5](#), [6](#)
- [14] Leo Grady. Random walks for image segmentation. *IEEE transactions on pattern analysis and machine intelligence*, 28(11):1768–1783, 2006. [2](#)
- [15] Jiaqi Gu, Hyoukjun Kwon, Dilin Wang, Wei Ye, Meng Li, Yu-Hsin Chen, Liangzhen Lai, Vikas Chandra, and David Z Pan. Multi-scale high-resolution vision transformer for semantic segmentation. In *Proceedings of the IEEE/CVF Conference on Computer Vision and Pattern Recognition*, pages 12094–12103, 2022. [2](#)
- [16] Varun Gulshan, Carsten Rother, Antonio Criminisi, Andrew Blake, and Andrew Zisserman. Geodesic star convexity for interactive image segmentation. In *2010 IEEE Computer Society Conference on Computer Vision and Pattern Recognition*, pages 3129–3136. IEEE, 2010. [2](#)
- [17] Agrim Gupta, Piotr Dollar, and Ross Girshick. Lvis: A dataset for large vocabulary instance segmentation. In *Proceedings of the IEEE/CVF conference on computer vision and pattern recognition*, pages 5356–5364, 2019. [5](#), [7](#)
- [18] Bharath Hariharan, Pablo Arbeláez, Lubomir Bourdev, Subhransu Maji, and Jitendra Malik. Semantic contours from inverse detectors. In *2011 international conference on computer vision*, pages 991–998. IEEE, 2011. [1](#), [5](#), [7](#)
- [19] Kaiming He, Xinlei Chen, Saining Xie, Yanghao Li, Piotr Dollár, and Ross Girshick. Masked autoencoders are scalable vision learners. *arXiv preprint arXiv:2111.06377*, 2021. [2](#), [3](#), [4](#)
- [20] Kaiming He, Xiangyu Zhang, Shaoqing Ren, and Jian Sun. Deep residual learning for image recognition. In *Proceedings of the IEEE conference on computer vision and pattern recognition*, pages 770–778, 2016. [1](#)
- [21] Won-Dong Jang and Chang-Su Kim. Interactive image segmentation via backpropagating refinement scheme. In *Proceedings of the IEEE/CVF Conference on Computer Vision and Pattern Recognition*, pages 5297–5306, 2019. [5](#)
- [22] Salman Khan, Muzammal Naseer, Munawar Hayat, Syed Waqas Zamir, Fahad Shahbaz Khan, and Mubarak Shah. Transformers in vision: A survey. *ACM computing surveys (CSUR)*, 54(10s):1–41, 2022. [2](#)
- [23] Yanghao Li, Hanzi Mao, Ross Girshick, and Kaiming He. Exploring plain vision transformer backbones for object detection. *arXiv preprint arXiv:2203.16527*, 2022. [2](#), [3](#), [4](#)
- [24] Zhuwen Li, Qifeng Chen, and Vladlen Koltun. Interactive image segmentation with latent diversity. In *Proceedings of the IEEE Conference on Computer Vision and Pattern Recognition*, pages 577–585, 2018. [5](#)
- [25] Tsung-Yi Lin, Piotr Dollár, Ross Girshick, Kaiming He, Bharath Hariharan, and Serge Belongie. Feature pyramid networks for object detection. In *Proceedings of the IEEE conference on computer vision and pattern recognition*, pages 2117–2125, 2017. [2](#), [3](#)

- [26] Tsung-Yi Lin, Michael Maire, Serge Belongie, James Hays, Pietro Perona, Deva Ramanan, Piotr Dollár, and C Lawrence Zitnick. Microsoft coco: Common objects in context. In *European conference on computer vision*, pages 740–755. Springer, 2014. 5, 7
- [27] Zheng Lin, Zheng-Peng Duan, Zhao Zhang, Chun-Le Guo, and Ming-Ming Cheng. Focuscut: Diving into a focus view in interactive segmentation. In *Proceedings of the IEEE/CVF Conference on Computer Vision and Pattern Recognition*, pages 2637–2646, 2022. 1, 2, 4, 5, 6, 8
- [28] Zheng Lin, Zhao Zhang, Lin-Zhuo Chen, Ming-Ming Cheng, and Shao-Ping Lu. Interactive image segmentation with first click attention. In *Proceedings of the IEEE/CVF Conference on Computer Vision and Pattern Recognition*, pages 13339–13348, 2020. 2, 5
- [29] Geert Litjens, Thijs Kooi, Babak Ehteshami Bejnordi, Arnaud Arindra Adiyoso Setio, Francesco Ciompi, Mohsen Ghafoorian, Jeroen AWM Van Der Laak, Bram Van Ginneken, and Clara I Sánchez. A survey on deep learning in medical image analysis. *Medical image analysis*, 42:60–88, 2017. 1
- [30] Qin Liu, Zhenlin Xu, Yining Jiao, and Marc Niethammer. isegformer: Interactive segmentation via transformers with application to 3d knee mr images. In *International Conference on Medical Image Computing and Computer-Assisted Intervention*, pages 464–474. Springer, 2022. 1, 5, 8
- [31] Qin Liu, Meng Zheng, Benjamin Planche, Srikrishna Karanam, Terrence Chen, Marc Niethammer, and Ziyang Wu. Pseudoclick: Interactive image segmentation with click imitation. *arXiv preprint arXiv:2207.05282*, 2022. 1, 2, 4, 5, 6
- [32] Ze Liu, Yutong Lin, Yue Cao, Han Hu, Yixuan Wei, Zheng Zhang, Stephen Lin, and Baining Guo. Swin transformer: Hierarchical vision transformer using shifted windows. In *Proceedings of the IEEE/CVF International Conference on Computer Vision*, pages 10012–10022, 2021. 1, 2
- [33] Kevis-Kokitsi Maninis, Sergi Caelles, Jordi Pont-Tuset, and Luc Van Gool. Deep extreme cut: From extreme points to object segmentation. In *Proceedings of the IEEE Conference on Computer Vision and Pattern Recognition*, pages 616–625, 2018. 2
- [34] David Martin, Charless Fowlkes, Doron Tal, and Jitendra Malik. A database of human segmented natural images and its application to evaluating segmentation algorithms and measuring ecological statistics. In *Proceedings Eighth IEEE International Conference on Computer Vision. ICCV 2001*, volume 2, pages 416–423. IEEE, 2001. 4, 5
- [35] Adam Paszke, Sam Gross, Francisco Massa, Adam Lerer, James Bradbury, Gregory Chanan, Trevor Killeen, Zeming Lin, Natalia Gimelshein, Luca Antiga, et al. Pytorch: An imperative style, high-performance deep learning library. *Advances in neural information processing systems*, 32, 2019. 6
- [36] Federico Perazzi, Jordi Pont-Tuset, Brian McWilliams, Luc Van Gool, Markus Gross, and Alexander Sorkine-Hornung. A benchmark dataset and evaluation methodology for video object segmentation. In *Proceedings of the IEEE conference on computer vision and pattern recognition*, pages 724–732, 2016. 4, 5, 8
- [37] Carsten Rother, Vladimir Kolmogorov, and Andrew Blake. " grabcut" interactive foreground extraction using iterated graph cuts. *ACM transactions on graphics (TOG)*, 23(3):309–314, 2004. 2, 4, 5
- [38] Dinggang Shen, Guorong Wu, and Heung-Il Suk. Deep learning in medical image analysis. *Annual review of biomedical engineering*, 19:221, 2017. 1
- [39] Konstantin Sofiiuk, Ilia Petrov, Olga Barinova, and Anton Konushin. f-brs: Rethinking backpropagating refinement for interactive segmentation. In *Proceedings of the IEEE/CVF Conference on Computer Vision and Pattern Recognition*, pages 8623–8632, 2020. 5, 6
- [40] Konstantin Sofiiuk, Ilia A Petrov, and Anton Konushin. Reviving iterative training with mask guidance for interactive segmentation. *arXiv preprint arXiv:2102.06583*, 2021. 1, 2, 4, 5, 6, 8
- [41] Robin Strudel, Ricardo Garcia, Ivan Laptev, and Cordelia Schmid. Segmenter: Transformer for semantic segmentation. In *Proceedings of the IEEE/CVF International Conference on Computer Vision*, pages 7262–7272, 2021. 2
- [42] Jingdong Wang, Ke Sun, Tianheng Cheng, Borui Jiang, Chaorui Deng, Yang Zhao, Dong Liu, Yadong Mu, Mingkui Tan, Xinggang Wang, et al. Deep high-resolution representation learning for visual recognition. *IEEE transactions on pattern analysis and machine intelligence*, 43(10):3349–3364, 2020. 2
- [43] Jiajun Wu, Yibiao Zhao, Jun-Yan Zhu, Siwei Luo, and Zhuowen Tu. Milcut: A sweeping line multiple instance learning paradigm for interactive image segmentation. In *Proceedings of the IEEE Conference on Computer Vision and Pattern Recognition*, pages 256–263, 2014. 1, 2
- [44] Enze Xie, Wenhao Wang, Zhiding Yu, Anima Anandkumar, Jose M Alvarez, and Ping Luo. Segformer: Simple and efficient design for semantic segmentation with transformers. *Advances in Neural Information Processing Systems*, 34:12077–12090, 2021. 2
- [45] Ning Xu, Brian Price, Scott Cohen, Jimei Yang, and Thomas Huang. Deep grabcut for object selection. *arXiv preprint arXiv:1707.00243*, 2017. 1, 2
- [46] Ning Xu, Brian Price, Scott Cohen, Jimei Yang, and Thomas S Huang. Deep interactive object selection. In *Proceedings of the IEEE conference on computer vision and pattern recognition*, pages 373–381, 2016. 2, 5
- [47] Ning Xu, Linjie Yang, Yuchen Fan, Dingcheng Yue, Yuchen Liang, Jianchao Yang, and Thomas Huang. Youtube-vos: A large-scale video object segmentation benchmark. *arXiv preprint arXiv:1809.03327*, 2018. 1
- [48] Yuhui Yuan, Rao Fu, Lang Huang, Weihong Lin, Chao Zhang, Xilin Chen, and Jingdong Wang. Hrformer: High-resolution vision transformer for dense predict. *Advances in Neural Information Processing Systems*, 34:7281–7293, 2021. 2
- [49] Shiyin Zhang, Jun Hao Liew, Yunchao Wei, Shikui Wei, and Yao Zhao. Interactive object segmentation with inside-outside guidance. In *Proceedings of the IEEE/CVF con-*

- ference on computer vision and pattern recognition*, pages 12234–12244, 2020. [1](#), [2](#)
- [50] Xiaosong Zhang, Yunjie Tian, Wei Huang, Qixiang Ye, Qi Dai, Lingxi Xie, and Qi Tian. Hivit: Hierarchical vision transformer meets masked image modeling. *arXiv preprint arXiv:2205.14949*, 2022. [4](#)
- [51] Sixiao Zheng, Jiachen Lu, Hengshuang Zhao, Xiatian Zhu, Zekun Luo, Yabiao Wang, Yanwei Fu, Jianfeng Feng, Tao Xiang, Philip HS Torr, et al. Rethinking semantic segmentation from a sequence-to-sequence perspective with transformers. In *Proceedings of the IEEE/CVF conference on computer vision and pattern recognition*, pages 6881–6890, 2021. [2](#)